Heliyon 7 (2021) e07169

Contents lists available at ScienceDirect

Heliyon

journal homepage: www.cell.com/heliyon

Research article

Adsorption of Malachite Green by extracellular polymeric substance of *Lysinibacillus* sp. SS1: kinetics and isotherms

Harshitha Kamath Miyar, Annapoorna Pai, Louella Concepta Goveas *

Department of Biotechnology Engineering, NMAM Institute of Technology, Nitte 574110, India

ARTICLE INFO

Keywords:
EPS
Lysinibacillus sp. SS1
Malachite Green
Adsorption kinetics

ABSTRACT

Use of novel biological materials as adsorbents for removal of xenobiotics is gaining significance owing to their exceptional advantages. An extracellular polymeric substance (EPS) produced by *Lysinibacillus* sp. SS1 had rough porous surface as observed by SEM analysis. Adsorption ability of EPS was estimated against various textile dyes such as Malachite Green (MG), Methyl Orange, Congo Red and Coomassie Blue. About 82% of MG (100 mg/L) was adsorbed onto 2.5 mg EPS within 30 min. Effect of MG concentration, EPS weight, agitation speed and incubation time on adsorption, studied by one factor at a time approach, revealed that adsorption was influenced by all factors. Maximum adsorption of 99.01 ± 0.61% was achieved at 100 mg/L MG, 10 mg EPS, 120 RPM in 75 min with maximum adsorption capacity of 247.5 mg/g. Kinetics was affected by MG and EPS amounts, with shift from pseudo first to pseudo second order with increase in concentration. Adsorption of MG by EPS of *Lysinibacillus* sp. SS1 was identified as unilayer chemisorption as it followed Langmuir isotherm with maximum adsorption capacity (Q_m) of 178.57 mg/g ($R^2 = 0.9889$). This is the first report on potential of EPS produced by *Lysinibacillus* sp. SS1 as novel biodegradable adsorbent with high efficacy of MG removal from aqueous solutions.

1. Introduction

The textile dye industry is one among the largest industries in India that contributes to severe environmental pollution due to discharge of untreated dyeing effluents [1]. Release of dyeing effluents cause dire consequences on ecosystems, human health, soil fertility and marine life due to genotoxicity, mutagenicity and carcinogenicity of dyes [2]. Different methods such as membrane separation processes, degradation, flocculation, precipitation and oxidation, used for dye wastewater treatment, are successful in dye removal, however, on application in large scale are expensive for developing countries like India [3]. Process of adsorption is extensively used for removal of dyes owing to its high efficiency and ease of use [4]. Adsorbents such as activated carbon, activated alumina, silica gel, zeolites etc used in wastewater treatment, are expensive and have a complicated regeneration process [5]. This has paved way for search of novel, cost effective and simple adsorbents with high dye removal efficiency.

Several biological materials such as lignocellulosic wastes, agricultural wastes, bacterial and fungal biomass have been studied extensively in adsorption of dyes from wastewaters and effluents [6, 7, 8]. Utilization of extracellular polymeric substances (EPS), i.e. high molecular weight microbial polymers, as novel bio-adsorbents is currently gaining popularity due to their biodegradability, eco-friendliness, high competence and non-toxic nature [9, 10]. When a novel material is used as an adsorbent, study of factors effecting the process, adsorption kinetics and equilibrium data must be essentially studied and identified. Rate of adsorption can be predicted by kinetics, which is the basis for design of an adsorption process [11].

The present work deals with the adsorption of Malachite Green (MG) dye by EPS produced by *Lysinibacillus* sp. SS1, isolated from automotive service station soil. This EPS, previously reported for its heavy metal adsorption abilities, is produced by bacteria in response to petroleum crude oil (PCO) stress [12]. MG, a highly toxic triarylmethane dye, used for various purposes, such as food, cloth and paper colorant and as

* Corresponding author.
E-mail address: goveas.louella@nitte.edu.in (L.C. Goveas).

https://doi.org/10.1016/j.heliyon.2021.e07169
Received 9 April 2021; Received in revised form 4 May 2021; Accepted 26 May 2021

biocide in aquaculture, causes serious health effects and environmental implications [13]. The effect of factors on adsorption of MG by EPS was studied using one factor at a time (OFAT) approach. Additionally, adsorption kinetics and isotherms were studied at various adsorbate and adsorbent concentrations. This is the first report on study of kinetics and isotherms of adsorption of MG by bacterial EPS.

2. Materials and methods

2.1. Bacterium, substrates and chemicals

Lysinibacillus sp. SS1 (GenBank: MW897754.1), used for production of EPS, was previously isolated from automotive service station soil [12]. MG was procured from Sisco Research Laboratories (SRL Pvt Ltd, Mumbai, Maharashtra, India). All other chemicals used in this work were of analytical grade.

2.2. EPS production, extraction and structural analysis

EPS was produced by growing *Lysinibacillus* sp. SS1 (10% v/v, 10^8 CFU/mL) in Bushnell Haas broth (g/L: $MgSO_4$:0.2, KH_2PO_4: 1.0, K_2HPO_4: 1.0, $CaCl_2$: 0.02, $FeCl_3$: 0.05, NH_4NO_3: 1.0) supplemented with 3.0% v/v PCO as sole carbon source. After incubation at 27 ± 2 °C at 80 RPM for 10 days, EPS was extracted and purified from cell free supernatant (CFS) as previously described [12]. Briefly, CFS was dispersed with cold ethanol (1:4) and kept at 4 °C overnight. The precipitated EPS was collected by centrifugation at 10,000 RPM for 15 min and extracted with chloroform-butanol (99%) mixture (2:1). Partially purified EPS was obtained on evaporation of solvent at 60 °C. The surface of purified EPS was visualized by subjecting it to Scanning Electron Microscopy (SEM) (Jeol JSM 6390LV), while the elemental composition was determined by energy dispersive X-ray analysis (EDS).

2.3. Screening of dyes for adsorption by purified EPS of Lysinibacillus sp. SS1

Aqueous solutions (25 ml) of MG, Methyl Orange (MO), Congo Red (CR) and Coomasie Blue (CB) containing 100 mg/L was incubated with 2.5 mg of EPS for 30 min at 80 RPM. Temperature and pH were maintained at 27 ± 2 °C and 6.0 respectively. Residual concentrations of MG, MO, CR and CB in the solution were determined by measuring absorbance spectrophotometrically at 620 nm, 470 nm, 485 nm and 560 nm respectively. Percentage adsorption of dyes was calculated as follows

$$\%Adsorption = \frac{Ci - Ct}{Ci} * 100. \quad (1)$$

Where C_i and C_t are the initial dye concentration and the dye concentration after 2 h respectively.

Amount of dye adsorbed by EPS was calculated as per the following

$$Qt = \frac{V(Ci - Ct)}{W} \quad (2)$$

Where Q_t = amount of dye adsorbed (mg/g), V is the total volume of the solution (L), Ci and C_t are the initial dye concentration and the dye concentration after 2 h respectively (mg/L) and W is the weight of EPS added (g).

2.4. Effect of factors on MG adsorption by purified EPS by OFAT approach

Effect of factors such as MG concentration, EPS weight, agitation speed and incubation time on adsorption of MG by purified EPS was studied by OFAT. In OFAT approach, effect of one factor is studied by its variation while maintaining others constant [14]. The level of factor at which maximum output is obtained is fixed while varying the next factor. Levels of factors were maintained as per Table 1 and % adsorption was calculated as per Eq. (1). Temperature and pH were maintained at 27 ± 2 °C and 6.0 respectively for all experiments. Adsorption capacity (mg/g) and % adsorption were calculated by performing experiments at level of factors where maximum adsorption was achieved.

2.5. Adsorption kinetics

Pseudo first order (PFO) and pseudo second order (PSO) models are models that are extensively used to describe kinetics of adsorption of contaminants from liquid systems [15]. The kinetics of adsorption depends on initial concentration of pollutant in the system. In the present study, linearised equations of PFO and PSO models were used to describe adsorption kinetics of MG at various concentrations (25 mg/L - 100 mg/L) for 2.5 mg purified EPS. Additionally, kinetics was studied at various weights of EPS (2.5 mg–10 mg) for 100 mg/L MG.

The linearised form of PFO model is given as follows

$$\log(Qe - Qt) = \log Qe - \left(\frac{k1}{2.303}\right)t \quad (3)$$

Where Q_e and Q_t = amount of MG adsorbed (mg/g) at equilibrium and time t respectively and k_1 (min^{-1}) is the pseudo-first-order rate constant [16, 17].

The linearised form of PSO model that describes chemisorption is given as follows

$$\frac{t}{Qt} = \frac{1}{k2Qe^2} + \frac{1}{Qe}t \quad (4)$$

Where k_2 (g/mg.min) is the pseudo-second-order rate constant [18, 19].

Mechanism of adsorption includes three steps i.e. transfer of adsorbate to the surface of adsorbent (film diffusion), transfer from surface to the active sites (intraparticle diffusion) and binding of adsorbate on the active sites [20]. In-order to ascertain if intraparticle diffusion was the rate limiting step, intraparticle diffusion model was used. The linearised form of this model is described as follows

Table 1. Adsorption of MG by various adsorbents.

Adsorbent	MG (mg/L)	% Adsorption	Time (min)	Kinetics	Isotherms	Reference
Silica/rice husk composite	200	97.11	-	PSO	Freundlich	[42]
Mesoporous magnetic biochar	100	98.9	20	PSO	Langmuir	[43]
EPS stabilized iron oxide nanoparticles	100	93.77	6	PFO	-	[44]
Cellulose nanofibrils aerogel	100	92	-	PSO	Langmuir	[45]
Azadirachta indica leaves	50	92.8	120	PSO	Langmuir	[46]
Pandoraea pulmonicola biomass	50	85.2	-	-	Langmuir	[47]
Bacillus cereus biomass	100	85	360	PSO	Langmuir	[48]
EPS of *Lysinibacillus* sp. SS1	100	99.01	75	PFO	Langmuir	*This study*

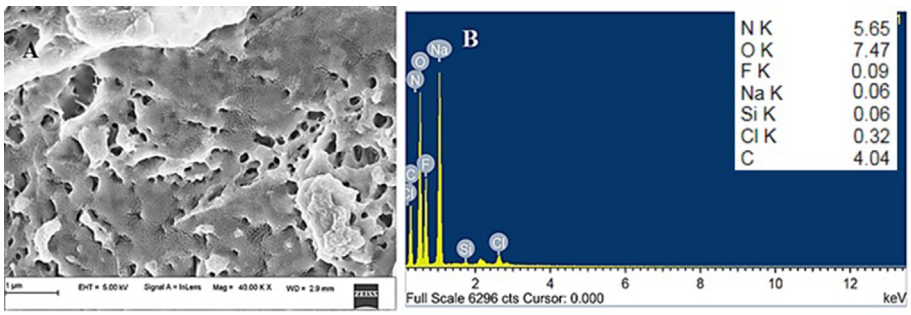

Figure 1. Surface and elemental composition of EPS produced by *Lysinibacillus* sp. SS1 visualized by SEM (A) and EDS (B) analysis.

$$Qt = kpt^{0.5} + C \quad (5)$$

Where *kp* (mg/g h) is the rate constant of this model. When a graph of Q_t versus $t^{0.5}$ is plotted, if a relationship is observed in the form of a straight line, it implies that intraparticle diffusion is rate limiting step, if multi-linear patterns are observed it indicates that the rate of the reaction is controlled by more than one step [21].

2.6. Adsorption isotherms

Adsorption isotherms are essential in design and optimization of adsorbent capacity for removal of pollutants from aqueous solutions [22]. They are curves relating equibrium amount of pollutant in solution (C_e) to the equilibrium amount of pollutant adsorbed (Q_e) [23]. The equilibrium study of MG adsorption by EPS of *Lysinibacillus* sp. SS1 was studied by three widely used adsorption isotherms namely, Freundlich, Langmuir and Temkin.

Eq. (6) depicts the linearized form of Freundlich isotherm

$$\ln Q_e = ln\, Kf + \frac{1}{n}\ln C_e. \quad (6)$$

Where K_f indicates maximum adsorption capacity (mg.L/g^2) and *n* ranges between 0 to 1 and determines the dependency of process on pressure [24, 25].

Linearized form of Langmuir isotherm is described by the following equation:

$$\frac{C_e}{Q_e} = \frac{1}{Q_m K_b} + \frac{C_e}{Q_m} \quad (7)$$

Where Q_m indicates the maximum adsorption capacity (mg/g) and K_b (L/mg) is the Langmuir constant [26].

The favourableness of adsorption can be described by a dimensionless constant R_L (Eq. (8))

$$R_L = \frac{1}{1 + K_b C_i} \quad (8)$$

If R_L values vary between 0 to 1, adsorption is favourable, whereas values greater than 1 indicate unfavourable adsorption [22].

Temkin isotherm is depicted by the following equation

$$Q_e = B \ln K_T + B \ln C_e \quad (9)$$

Where, K_T (L/mg) is the Temkin isotherm constant and B is constant related to sorption heat (J/mol) [27].

2.7. Statistical analysis

All the experiments of screening, OFAT, adsorption kinetics and isotherms were performed in triplicates. All the results are displayed as mean ± standard deviation.

3. Results and discussion

3.1. SEM-EDS analysis

The yield of purified EPS was 6.86 ± 0.14 g/L. The surface of purified EPS was visualized and characterised by SEM analysis as rough and partially porous (Figure 1). The presence of pores facilitates adsorption due to enhanced surface area. EDS analysis revealed the presence of carbon, oxygen and nitrogen confirming that the EPS was a glycolipid with protein moieties as reported earlier [12]. EPS-R040 produced by *Lactobacillus plantarum* had similar surface topology, which was effectively utilized in adsorption of methylene blue [9].

3.2. Screening of dyes for biosorption by purified EPS of Lysinibacillus sp. SS1

On addition of purified EPS (2.5 mg) to aqueous solution (25 mL) containing 100 mg/L of dyes, maximum % adsorption of 82.3 ± 0.17% was observed in 30 min for MG (Figure 2). Dyes MO and CB showed negligible adsorption while % adsorption of 13.71 ± 0.9% was observed for CR. The maximum adsorption capacity of EPS produced by *Lysinibacillus* sp. SS1 was calculated as 823.7 mg/g for MG, while the least adsorption capacity was 16.45 mg CB/g. Table 1 depicts the adsorption efficiency of MG by various adsorbents reported earlier. EPS of *Exiguobacterium* sp. VK1 showed biosorption capacity of 684.38 mg/g during adsorption of MG [28].

3.3. Effect of factors on MG adsorption by EPS of Lysinibacillus sp. SS1

3.3.1. Effect of MG concentration

The effect of MG concentration was varied from 100 to 300 mg/L on addition of 2.5 mg of EPS. After 30 min of agitation at 80 RPM, % adsorption was calculated. As the concentration of MG increased from 100 mg/L to 300 mg/L, the % adsorption reduced drastically from 82.3 ±

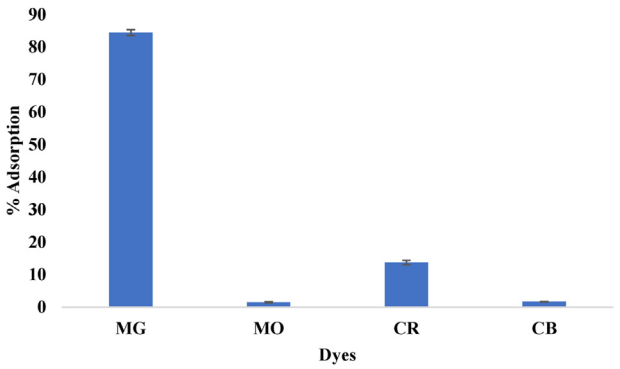

Figure 2. Adsorption of dyes by EPS produced by *Lysinibacillus* sp. SS1.

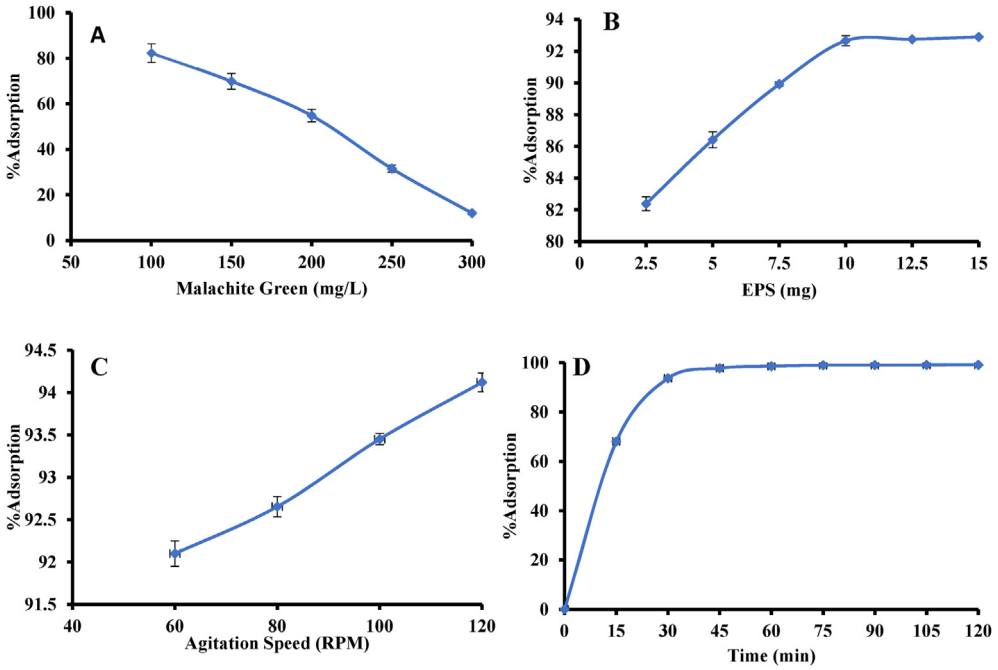

Figure 3. Effect of variation in MG (A); EPS (B); agitation speed (C) and time of incubation (D) on the adsorption of MG by EPS produced by *Lysinibacillus* sp. SS1.

0.81% to 11.94 ± 0.17%, indicating MG adsorption as a concentration-dependent process (Figure 3A). Several researchers have explained similar pattern on variation of dye concentration during adsorption with bio-adsorbents. Adsorption of methylene blue by corn husk decreased when concentration was increased from 20 mg/L to 100 mg/L [29]. On increase in MG concentration from 600 to 1500 mg/L the % adsorption by EPS of *Exiguobacterium* sp. VK1 reduced from 76% to 67% [28].

3.3.2. Effect of EPS weight

Adsorption was performed by variation of EPS weights (2.5–15.0 mg) while maintaining MG concentration at 100 mg/L, agitation speed of 80 RPM for 30 min. Adsorption increased from 82.3 ± 0.44% to 92.65 ± 0.31% on increase of EPS weight from 2.5 mg to 10 mg (Figure 3B). Increase in adsorbent amount means a greater number of interacting sites resulting in enhanced adsorption [30]. Further increase in EPS weight showed no significant change in % adsorption which is due to the fixed amount of adsorbate molecules (MG concentration = 100 mg/L). About 98–99% for adsorption of Reactive Blue and CR by coffee waste adsorbent was achieved at adsorbent weight 0.1 g with no change in further increase of weight [31].

3.3.3. Effect of agitation speed

Agitation speed plays an important role in solid liquid mass transfer mechanism and reduced boundary layer resistance while enhancing contact between adsorbate and adsorbent [32]. Agitation speed was varied from 60 RPM to 120 RPM to study its effect on adsorption of MG (100 mg/L) by EPS (10 mg) of *Lysinibacillus* sp. SS1 (Figure 3C). Adsorption increased with increase in agitation speed and was maximum at 120 RPM (% adsorption = 94.12 ± 0.11). Maximum adsorption of Eriochrome Black-T by titanium oxide was observed at agitation speed of 200 RPM [33]. EPS produced by *Lactobacillus plantarum* also showed increase in adsorption of methylene blue on increase in agitation speed from 0 to 100 RPM [9].

3.3.4. Effect of incubation time

Adsorption experiments were carried out by addition of 10 mg of EPS to aqueous solution (25 mL) of MG (100 mg/L) for 2 h at 120 RPM. % Adsorption was calculated every 15 min in order to estimate the effect of incubation time (Figure 3D). A rapid increase in adsorption was observed up to 30 min of incubation (93.23 ± 0.18%) after which a gradual increase up to 75 min (98.97 ± 0.69%) was noted. Equilibrium was attained after 75 min of incubation. Adsorption of methylene blue by *Exiguobacterium* sp. VK1 increased up to 90 min post which equilibrium was attained [28].

3.3.5. Adsorption at optimum conditions

Adsorption of MG by EPS of *Lysinibacillus* sp. SS1 was carried out at optimum conditions as obtained by OFAT studies i.e., 100 mg/L MG, 10 mg EPS weight, agitation speed 120 RPM and incubation time 75 min. Maximum % adsorption of 99.01 ± 0.61% was attained with fold increase of 1.2. The adsorption capacity was reduced to 247.5 mg/g from initial capacity of 1035 mg/g (section 3.1), due to increase in EPS weight (from 2.5 mg to 10 mg). Figures 4A and 4B depict the adsorption of MG by EPS at optimised conditions after 15 and 75 min of incubation respectively. After 75 min, complete decolourisation of aqueous solution can be visualised on comparison with the control.

3.4. Adsorption kinetics

The kinetics of adsorption of MG by EPS of *Lysinibacillus* sp. SS1 was studied by two models namely PFO and PSO. Kinetics of adsorption was compared at different MG concentrations (100 mg/L – 200 mg/L) using constant quantity of EPS (2.5 mg) (Figure 5). Although, PSO model showed good fit ($R^2 = 0.9853$), adsorption kinetics was best described by PFO model ($R^2 = 0.9971$) at 100 mg/L. At higher concentrations, the

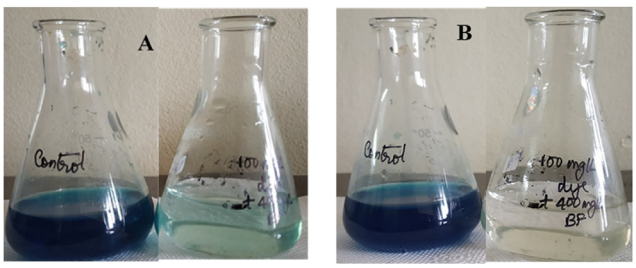

Figure 4. Decolorization of MG on addition of different weights of purified EPS produced by *Lysinibacillus* sp. SS1 after 30 min (A) and 75 min (B) of incubation.

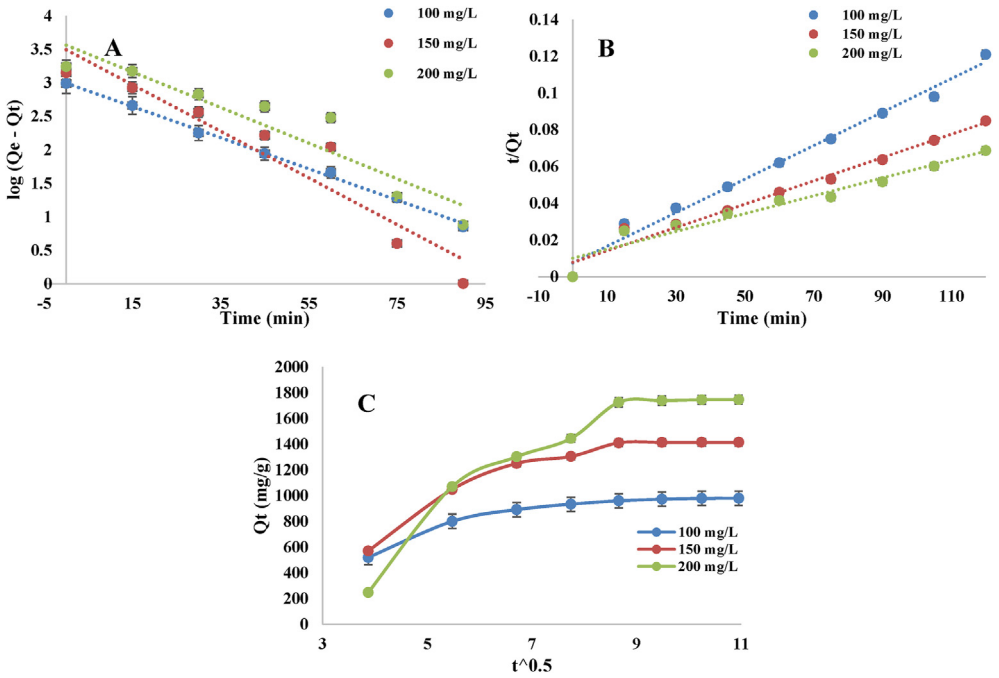

Figure 5. Kinetics of adsorption of different concentrations of MG (100–200 mg/L) by 2.5 mg EPS of *Lysinibacillus* sp. SS1: PFO (A); PSO (B) and intraparticle diffusion (C).

adsorption kinetics followed PSO model (Table 2), indicating adsorption of MG by EPS of *Lysinibacillus* sp. SS1 is concentration-dependent with surface adsorption being the rate controlling step [34]. Adsorption kinetics of methylene blue by EPS produced by *Lactobacillus plantarum* also shifted from PFO to PSO with increase in concentration from 50 mg/L to 100 mg/L [9]. Most of biosorption processes of dyes reported in literature follow PSO kinetics (Asfaram et al., [37]; Aksakal and Ucun, [36]; Ncibi et al., [35]). The PFO rate constant (k_1) was obtained as 0.053 min^{-1} at 100 mg/L, while k_2 values were 4.61E-05 g/mg.min and 2.47E-05 g/mg.min at 150 mg/L and 250 mg/L respectively. Adsorption of MG by *Yarrowia lipolityca* followed PSO kinetics with k_2 of 7E-04 g/mg.min [37].

Effect of adsorbent amount on adsorption kinetics of MG was studied by performing experiments with EPS weight of 2.5 mg, 5.0 mg and 10.0 mg at 100 mg/L MG (Figure 6). Adsorption followed PFO kinetics at 2.5 mg and 5.0 mg (R^2 = 0.9976 and 0.998), but at 10 mg EPS, adsorption was best described by PSO model (R^2 = 0.9976). These results reveal that adsorption kinetics is also affected by adsorbent amount along with the adsorbate. Adsorption rate constant (k_1) was obtained as 0.052 min^{-1} and 0.066 min^{-1} at 2.5 mg and 5.0 mg respectively, while k_2 values were 1.35E-03 g/mg.min at 10 mg.

The intraparticle diffusion model describes the diffusion of adsorbate into the porous matrix of the adsorbent [38]. Multilinear intraparticle diffusion curves were observed in all cases implying that adsorption process was controlled by intraparticle diffusion till 30 min beyond which it was governed by multiple steps (Figure 5C;Figure 6C).

3.5. Adsorption isotherms

The equibrium data of adsorption of MG by EPS of *Lysinibacillus* sp. SS1 was modelled by Freundlich, Langmuir and Temkin isotherms (Figure 7). Among three isotherms tested, the EPS mediated biosorption was best described by Langmuir isotherm (R^2 = 0.9889) indicating that MG gets adsorbed on the homogenous EPS surface as a monolayer [39]. Most of the adsorption processes involving MG have been reported to follow Langmuir isotherm (Table 1). The binding of MG onto the EPS was strong to prevent displacement of MG along from the surface indicating that the process is chemisorption [40]. These results match with the findings of kinetic studies. Adsorption of uranium by EPS of *Synechococcus elongatus* also followed Langmuir isotherm with R^2 of 0.988 [41]. The maximum adsorption capacity (Q_m) was calculated as 178.57 mg/g which was comparable to the adsorption capacity at optimized

Table 2. Kinetics of Adsorption of MG by EPS produced by *Lysinibacillus* sp. SS1.

Kinetic Parameters	MG (mg/L)			EPS (mg)		
	100	150	200	2.5	5	10
Qe, exp (mg/g)	979.031	1414.6	1746.51	979.031	490.2	247.623
Pseudo-first Order						
k_1 (min^{-1})	**0.053**	0.08	0.061	**0.052**	**0.066**	0.0794
Qe, cal (mg/g)	**990.375**	3122.48	3657.1	**951.91**	**471.3**	201.1
R^2	**0.9971**	0.9023	0.8813	**0.9976**	**0.998**	0.9585
Pseudo-Second Order						
k_2 (g/mg.min)	1.00E-03	**4.61E-05**	**2.47E-05**	1.00E-03	4.65E-04	**1.35E-03**
Qe, cal (mg/g)	1111.11	**1666.67**	**2000**	1111.11	500	**256.41**
R^2	0.9853	**0.9729**	**0.9413**	0.9853	0.9938	**0.9976**

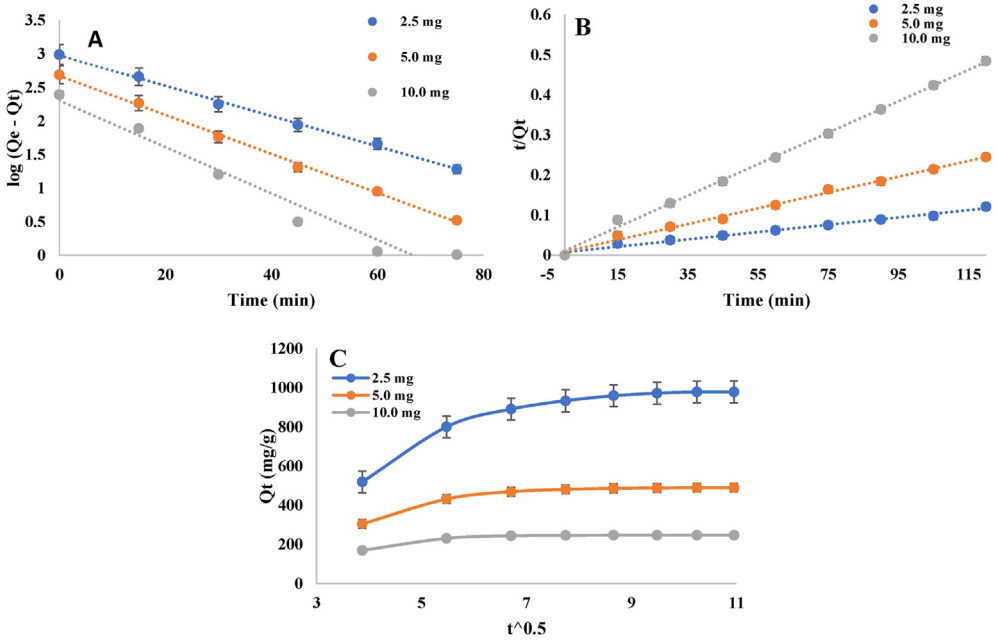

Figure 6. Kinetics of adsorption of 100 mg/L MG by different weights of EPS (2.5–10 mg) of *Lysinibacillus* sp. SS1: PFO (A); PSO (B) and intraparticle diffusion (C).

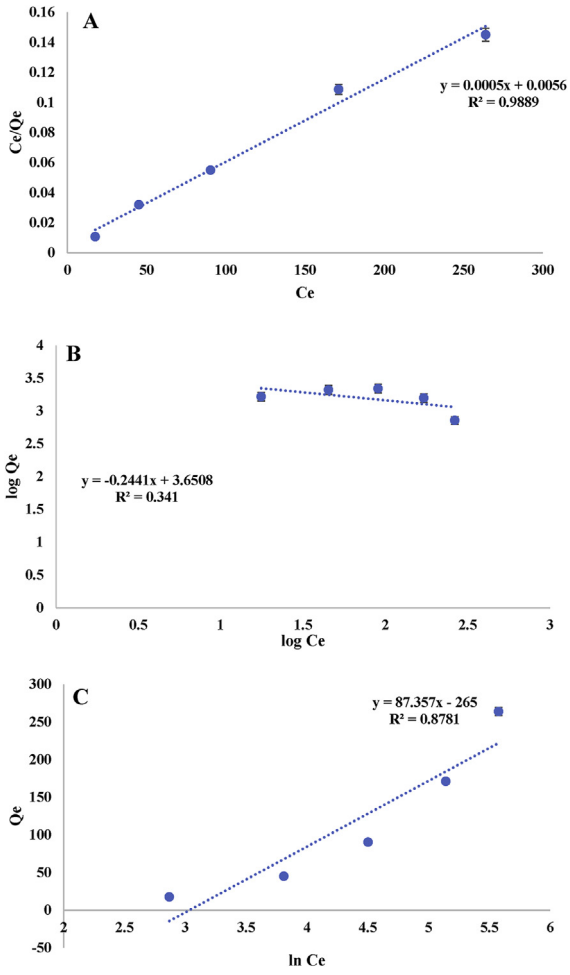

Figure 7. Isotherms describing equilibrium studies of 100 mg/L MG adsorption by EPS (10 mg) of *Lysinibacillus* sp. SS1: Langmuir isotherm (A), Freundlich isotherm (B) and Temkin isotherm (C).

conditions (247.5 mg/g) (Table 1). The value of Langmuir constant (K_b) was observed as 0.089 L/mg which was comparable with reports in literature [9]. R_L values varied from 0.036 to 0.101 for MG concentrations used in this study (100 mg/L to 300 mg/L) indicating that adsorption of MG by EPS of *Lysinibacillus* sp. SS1 was spontaneous and favourable.

4. Conclusions

Availability of novel bio adsorbents and extensive knowledge of adsorption equilibrium and kinetics is essential for removal of contaminants from polluted water. This present study portrays the ability of a previously reported novel lipoprotein heavy metal adsorbing bacterial EPS in dye adsorption. The study of kinetics and isotherms depicted that process of MG removal was due to chemical binding which was affected by its initial concentration. EPS had a maximum adsorption capacity of 247.5 mg/g for 100 mg/L MG indicating its high appropriateness for treatment of dye wastewaters polluted with MG.

Declarations

Author contribution statement

Harshitha Kamath Miyar & Annapoorna Pai: Performed the experiments; Analyzed and interpreted the data.

Louella Concepta Goveas: Conceived and designed the experiments; Analyzed and interpreted the data; Contributed reagents, materials, analysis tools or data; Wrote the paper.

Funding statement

This research did not receive any specific grant from funding agencies in the public, commercial, or not-for-profit sectors.

Data availability statement

No data was used for the research described in the article.

Declaration of interests statement

The authors declare no conflict of interest.

Additional information

No additional information is available for this paper.

References

[1] M. Islam, M. Mostafa, Textile dyeing effluents and environment concerns, J. Environ. Sci. Nat. Resour. 11 (2019) 131–144.
[2] N. Puvaneswari, J. Muthukrishnan, P. Gunasekaran, Toxicity assessment and microbial degradation of azo dyes, Indian J. Exp. Biol. 44 (2006) 618–626.
[3] J.F. Gao, Q. Zhang, J.H. Wang, X.L. Wu, S.Y. Wang, Y.Z. Peng, Contributions of functional groups and extracellular polymeric substances on the biosorption of dyes by aerobic granules, Bioresour. Technol. 102 (2011) 805–813.
[4] M. Agarwal Renu, K. Singh, Heavy metal removal from wastewater using various adsorbents: a review, J. Water Reuse Desalin. 7 (2017) 387–419.
[5] A. Abdolali, W.S. Guo, H.H. Ngo, S.S. Chen, N.C. Nguyen, K.L. Tung, Typical lignocellulosic wastes and by-products for biosorption process in water and wastewater treatment: a critical review, Bioresour. Technol. 160 (2014) 57–66.
[6] S. Celik, N. Duman, F. Sayin, S. Tunali Akar, T. Akar, Microbial cells immobilized on natural biomatrix as a new potential ecofriendly biosorbent for the biotreatment of reactive dye contamination, J. Water Process Eng. 39 (2021) 101731.
[7] A. Azari, M. Noorisepehr, E. Dehganifard, K. Karimyan, S.Y. Hashemi, E.M. Kalhori, R. Norouzi, S. Agarwal, V.K. Gupta, Experimental design, modeling and mechanism of cationic dyes biosorption on to magnetic chitosan-lutaraldehyde composite, Int. J. Biol. Macromol. 131 (2019) 633–645.
[8] S. Rangabhashiyam, S. Lata, P. Balasubramanian, Biosorption characteristics of methylene blue and malachite green from simulated wastewater onto *Carica papaya* wood biosorbent, Surf. Interf. 10 (2018) 197–215.
[9] C. Li, D. Chen, J. Ding, Z. Shi, A novel hetero-exopolysaccharide for the adsorption of methylene blue from aqueous solutions: isotherm, kinetic, and mechanism studies, J. Clean. Prod. 265 (2020) 121800.
[10] U. Tahir, A. Yasmin, Role of bacterial extracellular polymeric substances (EPS) in uptake and accumulation of co-contaminants, Int. J. Environ. Sci. Technol. 16 (2019) 8081–8092.
[11] W. Wang, J. Wang, Comparative evaluation of sorption kinetics and isotherms of pyrene onto microplastics, Chemosphere 193 (2018) 567–573.
[12] H. Kamath Miyar, A. Pai, S.P. Sajankila, L.C. Goveas, Extracellular polymeric substance produced by *Lysinibacillus* sp. SS1 in response to petroleum crude oil stress facilitates removal of heavy metals from aqueous solutions, Philipp. J. Sci. 149 (2020) 1217–1225.
[13] S. Srivastava, R. Sinha, D. Roy, Toxicological effects of malachite green, Aquat. Toxicol. 66 (2004) 319–329.
[14] L.C. Goveas, J. Menezes, A. Salian, A. Krishna, M. Alva, B. Basavapattan, S.P. Sajankila, Petroleum hydrocarbon degradation in soil augmented with used engine oil by novel *Pantoea wallisii* SS2: optimisation by response surface methodology, Biocatal. Agric. Biotechnol. 25 (2020) 101614.
[15] K.L. Tan, B.H. Hameed, Insight into the adsorption kinetics models for the removal of contaminants from aqueous solutions, J. Taiwan Inst. Chem. Eng. 74 (2017) 25–48.
[16] S. Sharma, A. Hasan, N. Kumar, L.M. Pandey, Removal of methylene blue dye from aqueous solution using immobilized *Agrobacterium fabrum* biomass along with iron oxide nanoparticles as biosorbent, Environ. Sci. Pollut. Res. 25 (2018) 21605–21615.
[17] M. Alimohammady, M. Jahangiri, F. Kiani, H. Tahermansouri, Design and evaluation of functionalized multi-walled carbon nanotubes by 3-aminopyrazole for the removal of Hg(II) and As(III) ions from aqueous solution, Res. Chem. Intermed. 44 (2018) 69–92.
[18] Q. Huang, X. Lin, L. Xiong, C. Huang, H. Zhang, M. Luo, L. Tian, X. Chen, Equilibrium, kinetic and thermodynamic studies of acid soluble lignin adsorption from rice straw hydrolysate by a self-synthesized macro/mesoporous resin, RSC Adv. 7 (2017) 23896–23906.
[19] M. Alimohammady, M. Jahangiri, F. Kiani, H. Tahermansouri, Preparation and characterization of functionalized MWCNTs-COOH with 3-amino-5-phenylpyrazole as an adsorbent and optimization study using central composite design, Carbon Lett. 29 (2019) 1–20.
[20] M. Arabloo, M.H. Ghazanfari, D. Rashtchian, Wettability modification, interfacial tension and adsorption characteristics of a new surfactant: implications for enhanced oil recovery, Fuel 185 (2016) 199–210.
[21] A. Pholosi, E.B. Naidoo, A.E. Ofomaja, Intraparticle diffusion of Cr(VI) through biomass and magnetite coated biomass: a comparative kinetic and diffusion study, S. Afr. J. Chem. Eng. 32 (2020) 39–55.
[22] N. Ayawei, A.N. Ebelegi, D. Wankasi, Modelling and interpretation of adsorption isotherms, J. Chem. 2017 (2017) 1–11.
[23] N. El Ouahedy, M. Zbair, S. Ojala, R. Brahmi, L. Pirault-Roy, Porous carbon materials derived from olive kernels: application in adsorption of organic pollutants, Environ. Sci. Pollut. Res. 27 (2020) 29967–29982.
[24] K. Walsh, S. Mayer, D. Rehmann, T. Hofmann, K. Glas, Equilibrium data and its analysis with the Freundlich model in the adsorption of arsenic(V) on granular ferric hydroxide, Separ. Purif. Technol. 243 (2020) 116704.
[25] M. Alimohammady, M. Ghaemi, Adsorptive removal of Hg2+ from aqueous solutions using amino phenyl-pyrazole-functionalized graphene oxide, Carbon Lett. 30 (2020) 493–508.
[26] E.C. Nnadozie, P.A. Ajibade, Data for experimental and calculated values of the adsorption of Pb(II) and Cr(VI) on APTES functionalized magnetite biochar using Langmuir, Freundlich and Temkin equations, Data Br. 32 (2020) 106292.
[27] M. Alimohammady, M. Jahangiri, F. Kiani, H. Tahermansouri, A new modified MWCNTs with 3-aminopyrazole as a nanoadsorbent for Cd(II) removal from aqueous solutions, J. Environ. Chem. Eng. 5 (2017) 3405–3417.
[28] R. Kalpana, M. Maheshwaran, E. Vimali, M.R. Soosai, C.S. Shivamathi, I.G. Moorthy, B. Ashokkumar, P. Varalakshmi, Decolorization of textile dye by halophilic Exiguobacterium sp.VK1: biomass and exopolysaccharide (EPS) enhancement for bioremediation of Malachite Green, ChemistrySelect 5 (2020) 8787–8797.
[29] O.M. Paşka, C. Pəcurariu, S.G. Muntean, Kinetic and thermodynamic studies on methylene blue biosorption using corn-husk, RSC Adv. 4 (2014) 62621–62630.
[30] S. Banerjee, M.C. Chattopadhyaya, Adsorption characteristics for the removal of a toxic dye, tartrazine from aqueous solutions by a low cost agricultural by-product, Arab. J. Chem. 10 (2017) S1629–S1638.
[31] S. Wong, N.A. Ghafar, N. Ngadi, F.A. Razmi, I.M. Inuwa, R. Mat, N.A.S. Amin, Effective removal of anionic textile dyes using adsorbent synthesized from coffee waste, Sci. Rep. 10 (2020) 1–13.
[32] W.T. Tsai, H.C. Hsu, T.Y. Su, K.Y. Lin, C.M. Lin, T.H. Dai, The adsorption of cationic dye from aqueous solution onto acid-activated andesite, J. Hazard Mater. 147 (2007) 1056–1062.
[33] B. Priyadarshini, P.P. Rath, S.S. Behera, S.R. Panda, T.R. Sahoo, P.K. Parhi, Kinetics, thermodynamics and isotherm studies on adsorption of Eriochrome Black-T from aqueous solution using rutile titanium oxide, Mater. Sci. Eng. 310 (2017) 1–15.
[34] W. Plazinski, J. Dziuba, W. Rudzinski, Modeling of sorption kinetics: the pseudo-second order equation and the sorbate intraparticle diffusivity, Adsorption 19 (2013) 1055–1064.
[35] M.C. Ncibi, B. Mahjoub, M. Seffen, Kinetic and equilibrium studies of methylene blue biosorption by *Posidonia oceanica* (L.) fibres, J. Hazard Mater. 139 (2007) 280–285.
[36] O. Aksakal, H. Ucun, Equilibrium, kinetic and thermodynamic studies of the biosorption of textile dye (Reactive Red 195) onto *Pinus sylvestris* L, J. Hazard Mater. 181 (2010) 666–672.
[37] A. Asfaram, M. Ghaedi, G.R. Ghezelbash, F. Pepe, Application of experimental design and derivative spectrophotometry methods in optimization and analysis of biosorption of binary mixtures of basic dyes from aqueous solutions, Ecotoxicol. Environ. Saf. 139 (2017) 219–227.
[38] W. Bin Lu, J.J. Shi, C.H. Wang, J.S. Chang, Biosorption of lead, copper and cadmium by an indigenous isolate *Enterobacter* sp. J1 possessing high heavy-metal resistance, J. Hazard Mater. 134 (2006) 80–86.
[39] S. Khodadoust, M. Ghaedi, R. Sahraei, A. Daneshfar, Application of experimental design for removal of sunset yellow by copper sulfide nanoparticles loaded on activated carbon, J. Ind. Eng. Chem. 20 (2014) 2663–2670.
[40] A. Dabrowski, Adsorption - from theory to practice, Adv. Colloid Interface Sci. 93 (2001) 135–224.
[41] V. Rashmi, A. Darshana, T. Bhuvaneshwari, S.K. Saha, L. Uma, D. Prabaharan, Uranium adsorption and oil emulsification by extracellular polysaccharide (EPS) of a halophilic unicellular marine cyanobacterium *Synechococcus elongatus* BDU130911, Curr. Res. Green Sustain. Chem. 4 (2021) 100051.
[42] M. Mobarak, E.A. Mohamed, A.Q. Selim, M.F. Eissa, M.K. Seliem, Experimental results and theoretical statistical modeling of malachite green adsorption onto MCM–41 silica/rice husk composite modified by beta radiation, J. Mol. Liq. 273 (2019) 68–82.
[43] A.S. Eltaweil, H. Ali Mohamed, E.M. Abd El-Monaem, G.M. El-Subruiti, Mesoporous magnetic biochar composite for enhanced adsorption of malachite green dye: characterization, adsorption kinetics, thermodynamics and isotherms, Adv. Powder Technol. 31 (2020) 1253–1263.
[44] B. Sharma, S. Menon, S. Mathur, N. Kumari, V. Sharma, Decolorization of malachite green dye from aqueous solution using biosurfactant-stabilized iron oxide nanoparticles: process optimization and reaction kinetics, Int. J. Environ. Sci. Technol. (2020) 1–14.
[45] F. Jiang, D.M. Dinh, Y. Lo Hsieh, Adsorption and desorption of cationic malachite green dye on cellulose nanofibril aerogels, Carbohydr. Polym. 173 (2017) 286–294.
[46] S.A. Odoemelam, U.N. Emeh, N.O. Eddy, Experimental and computational chemistry studies on the removal of methylene blue and malachite green dyes from aqueous solution by neem (*Azadirachta indica*) leaves, J. Taibah Univ. Sci. 12 (2018) 255–265.
[47] C.Y. Chen, J.T. Kuo, C.Y. Cheng, Y.T. Huang, I.H. Ho, Y.C. Chung, Biological decolorization of dye solution containing Malachite Green by *Pandoraea pulmonicola* YC32 using a batch and continuous system, J. Hazard Mater. 172 (2009) 1439–1445.
[48] J. Nath, L. Ray, Biosorption of Malachite Green from aqueous solution by dry cells of *Bacillus cereus* M116 (MTCC 5521), J. Environ. Chem. Eng. 3 (2015) 386–394.